Nonmagnetic ions enhance magnetic order in the ludwigite $Co_5Sn(O_2BO_3)_2$

Cynthia P. Contreras Medrano,[1] D. C. Freitas,[2] D. R. Sanchez,[1] C. B. Pinheiro,[3] G. G. Eslava,[4] L. Ghivelder,[4] and M. A. Continentino[2]

[1]*Instituto de Física, Universidade Federal Fluminense, Campus da Praia Vermelha, 24210-346, Niterói, RJ, Brazil*

[2]*Centro Brasileiro de Pesquisas Físicas, Rua Dr. Xavier Sigaud, 150 - Urca, 22290-180, Rio de Janeiro, RJ, Brazil*

[3]*Departamento de Física, Instituto de Ciências Exatas, Universidade Federal de Minas Gerais, Campus da Pampulha, Caixa Postal 702, 30123-970, Belo Horizonte, MG, Brazil*

[4]*Instituto de Física, Universidade Federal do Rio de Janeiro, Caixa Postal 68528, 21945-970, Rio de Janeiro, RJ, Brazil*

(Received 29 November 2014; revised manuscript received 19 January 2015; published 4 February 2015)

The ludwigite $Co_5Sn(O_2BO_3)_2$ was studied using x-ray diffraction, Mössbauer spectroscopy, and magnetic and thermodynamic measurements. This material belongs to a family of oxyborates which presents low-dimensional subunits in the form of three-leg ladders in its structure. The subunits confer to these materials a strong anisotropy in their exchange interactions that provide to the ludwigites several interesting magnetic properties, from partial ordering to spin-glass states. Despite being doped by nonmagnetic ions, $Co_5Sn(O_2BO_3)_2$ has long-range magnetic order below 82 K which is, surprisingly, the highest critical temperature found so far in the ludwigites. This record can be explained by the absence of double-exchange interactions, usually present in the ludwigites and that gives rise to strong competition. In this paper we study the magnetic and structural properties of $Co_5Sn(O_2BO_3)_2$ and compare our results with those obtained in other cobalt ludwigites.

DOI: 10.1103/PhysRevB.91.054402 PACS number(s): 75.50.−y, 75.47.Lx, 75.60.−d, 75.30.Kz

I. INTRODUCTION

The anhydrous oxyborates have, in general, the metal ions in octahedral coordination with the oxygen and the boron in the center of triangles. In these materials the metal ions form substructures such as ribbons, ladders, and planes which confer strong anisotropy to the exchange interactions [1]. They are good examples of strongly correlated systems of low dimensionality with interesting physical properties. Among these, we mention the charge ordering in the ludwigite $Fe_3O_2BO_3$ [2,3] and in the warwickites Fe_2OBO_3 [4–6] and Mn_2OBO_3 [7], the partial magnetic ordering in the ludwigites $Fe_3O_2BO_3$ [8,9] and $CoFe_2O_2BO_3$ [10], the random singlet phase in the warwickite $MgTiOBO_3$ [11], and the two-dimensional antiferromagnetic magnons in the hulsite $Co_{5.52}Sb_{0.48}(O_2BO_3)_2$ [12].

Some oxyborates adopting the ludwigite-type structure have recently been studied mainly due to two interesting properties found in the $Fe_3O_2BO_3$ system cited above: a charge-ordering phenomenon and the existence of two magnetic subsystems ordering independently at different temperatures and in orthogonal directions. The only other known homometallic ludwigite is $Co_3O_2BO_3$ [13,14] and these discoveries in the Fe ludwigite motivated studies hoping to find similar behavior in this system. However, charge ordering was not found in this material [13] and the partial magnetic ordering was found only in Co ludwigites containing Fe^{3+} ions.

In pure $Co_3O_2BO_3$ or in a mixture with magnetic atoms such as iron $Co_{3-x}Fe_xO_2BO_3$ [10,15] ferromagnetic interactions are more important than in the iron-based ludwigites. In an effort to understand the complex magnetic behavior of all these materials, different groups started to study cobalt ludwigites containing nonmagnetic ions $Co_5Ti(O_2BO_3)_2$ [16], $CoMgGaO_2BO_3$ [17], and $Co_{3-x}Ga_xO_2BO_3$ [18]. In these compounds the magnetic behavior is weaker, in the sense of smaller ordering temperatures, and can even be destroyed by the introduction of nonmagnetic ions. In this paper we study the Sn-doped $Co_5Sn(O_2BO_3)_2$ ludwigite and show that, surprisingly, in this material the magnetic behavior is favored by the substitution of Co by the nonmagnetic Sn ion. This is evidenced by the higher Néel temperature (T_N) of the doped system. To the best of our knowledge this is the highest critical temperature, where the whole system orders magnetically, among the ludwigites. It is smaller only compared to the partial magnetic ordering of the Fe^{3+} in the ludwigites. The present work reports the results of x-ray diffraction, ac susceptibility, magnetization, Mössbauer spectroscopy, and specific heat for $Co_5Sn(O_2BO_3)_2$. We discuss these results and compare them with those obtained previously in other investigated cobalt ludwigites.

II. EXPERIMENTAL

A. Synthesis

The crystals were synthesized from a 5:1:2:10 molar mixture of $CoO : SnO_2 : HBO_3 : Na_2B_4O_7$, respectively. The mixture was heated at 1100 °C for 24 hours and cooled down to 600 °C for 48 hours. Then the oven was turned off. The bath was dissolved in hot water and the crystals cleaned in ultrasonic bath at 50 °C. Needle-shaped black crystals up to 3 mm in length were obtained.

B. Structural characterization

A single-crystal x-ray diffraction was done using an Xcalibur Atlas Gemini ultradiffractometer with graphite monochromated Mo Kα radiation ($\lambda = 0.71073$ Å). Low-temperature measurements were made using an Oxford Cryosystems device. The cell refinements were performed using the software CrysAlisPro [19]. Data were collected up to 75.5° in 2θ. Analytical numeric absorption correction using a multifaceted crystal model was applied [20]. The structure was solved and refined using the software SHELXS-97 [21] and SHELXL-97 [22], respectively. The tables were

TABLE I. Crystal data and structure refinement of $Co_5Sn(O_2BO_3)_2$.

Empirical formula from x-ray analysis	$Co_{5.07}Sn_{0.93}B_2O_{10}$
Formula weight	591.08 g/mol
Wavelength	0.717073 Å
Crystal size	$0.4567 \times 0.1511 \times 0.0550$ mm^3
Temperature	110 K
Crystal system	orthorhombic
Space group	(No. 55) *Pbam*
Unit cell dimension $a =$	9.4216(3) Å
$b =$	12.3281(2) Å
$c =$	3.10109(1) Å
Volume	360.194(2) Å^3
Z	2
Density (calculated)	5.450 Mg/m^3
Absorption coefficient	14.638/mm
$F(000)$	547
θ range	2.72° to 37.75°
Index range $h =$	−15, 16
$k =$	−21, 21
$l =$	−5, 5
Reflections collected	13669
Independent reflections	1070
R(int)	0.0422
Completeness to $\theta = 37.752$	96.9%
Absorption correction	analytic
Max/min transmission	0.481/0.063
Refinement method	full-matrix least squares on F^2
Data/restraints/parameters	1070/0/59
Goodness of fit on F^2	1.331
Final R indices $[I > 2\sigma(I)]$	$R1 = 0.0168$, $wR2 = 0.0364$
R indices (all data)	$R1 = 0.0204$, $wR2 = 0.0377$
Extinction coefficient	0.0130(4)
Largest difference peak	0.825 e Å^{-3}
Largest difference hole	−0.713 e Å^{-3}

generated by WinGX [23]. All atoms were clearly solved and full-matrix least-squares refinement procedures on F^2 with anisotropic thermal parameters were carried on using SHELXL-97. Crystal data, data collection parameters, and structure refinement data are summarized in Table I.

The structure was solved in analogous experimental conditions at 293 K and 110 K in order to observe any eventual conformational change with temperature. No evidence for any phase transition was found above 110 K. Figure 1 shows a schematic structure of the ludwigites projected along the c axis together with the polyhedra centered at metal ions. We remark that the complete structure, exception for the boron ions, may be obtained from the two three-leg ladder subunits formed respectively by the metal sites 4-2-4 and 3-1-3. The purity of the samples was confirmed by powder x-ray diffraction and the presence of the Sn in the compound by energy-dispersive x-ray spectroscopy (EDS) (not shown). The sites 1, 2, and 3 are exclusively occupied by Co atoms. The site 4 is occupied randomly by Sn and Co ions in a proportion of 0.46:0.54. Despite having almost the same

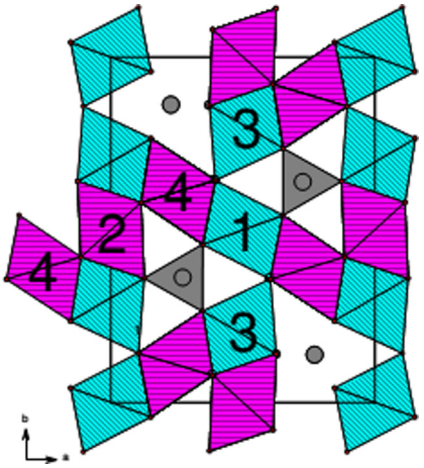

FIG. 1. (Color online) The schematic structure of the ludwigites projected along the c axis. The oxygen polyhedra centered on the metal ions are shown. The numbers indicate nonequivalent crystallographic metallic sites and the lines indicate the a and b axes of the unit cell. The subunits formed by the octahedra around sites 4-2-4 and 3-1-3 are emphasized by different colors. The boron ions (gray spheres) have trigonal coordination. This figure was generated by the Diamond 2.1e software [24].

proportion we did not see additional peaks indicating some kind of long-range order from the Sn and Co ions in this site. Contrary to the other nonmagnetic ions in the cobalt heterometallic structures, the Sn occupies only one site of the lattice. So the chemical composition of our sample, obtained from x-ray analysis, is $Co_{5.07}Sn_{0.93}(O_2BO_3)_2$. Table II shows the fractional coordinates and the site occupation factor. The bond lengths in this compound are shown in Table III. The intermetallic distance and also the distance between the metal and oxygen atoms in the octahedra are higher compared to the other cobalt ludwigites. From the M-O distances given in Table III, we may find the oxidation numbers for the Co ions in each lattice site by using the bond valence sum calculations. We applied the formulas given by Wood and Palenik [25] for

TABLE II. Fractional coordinates, site occupation factor (SOF), and the equivalent isotropic displacement parameters (Å$^2 \times 10^3$) for $Co_5Sn(O_2BO_3)_2$. U(eq) is defined as one third of the trace of the orthogonalized U_{ij} tensor. The SOF values must be multiplied by the factor 8 in order to obtain the number of atoms in the unit cell [26].

Site	x/a	y/b	z/c	SOF	U (eq)
Co(1)	0	0	1/2	1/4	6(1)
Co(2)	0	1/2	0	1/4	9(1)
Co(3)	0.0015(1)	0.2810(1)	1/2	1/2	6(1)
Co(4)	0.2397(1)	0.1151(1)	0	0.267	4(1)
Sn(4)	0.2405(1)	0.1161(1)	0	0.233	4(1)
O(1)	0.1520(1)	−0.0420(1)	0	1/2	7(1)
O(2)	0.1045(2)	0.1429(1)	1/2	1/2	7(1)
O(3)	0.1258(2)	0.3599(1)	0	1/2	7(1)
O(4)	−0.1143(2)	0.4210(1)	1/2	1/2	9(1)
O(5)	−0.1528(1)	0.2356(2)	0	1/2	7(1)
B	0.2723(2)	0.3618(2)	0	1/2	7(1)

TABLE III. Selected bond lengths in Å for $Co_5Sn(O_2BO_3)_2$. The subscripts are the symmetry codes: $(i)\ -x+1/2, y+1/2, -z$; $(ii)\ x+1/2, -y+1/2, z$; $(iii)\ x, y, z-1$; $(iv)\ -x, 1-y, z$; $(v)\ -1/2+x, 1/2-y, 1-z$.

Co1-O1	2.1733(9)	Co4-O1	2.1052(2)
Co1-O2	2.0177(1)	B-O3	1.381(3)
Co2-O3	2.0949(1)	B-$O1_i$	1.384(2)
Co2-O4	2.1243(1)	B-$O5_{ii}$	1.392(3)
Co3-O2	1.9596(1)	Co2-Co4	2.8338(1)
Co3-O4	2.0413(2)	Co3-Co2	3.1135(2)
Co3-O3	2.1725(1)	Co3-$Co1_v$	3.4642(3)
Co3-O5	2.1983(1)	Co4-Co1	3.0849(9)
Co4-$O2_{iii}$	2.0356(1)	Co4-$Co3_{iv}$	31829(9)
Co4-$O5_{ii}$	2.1009(2)		
Co4-$O4_{ii}$	2.1204(1)		

the oxidation number Z_j for the Co ion on site j,

$$Z_j = \sum_i s_{ij}, \tag{1}$$

where $s_{ij} = \exp[(R_0 - r_{ij})/b]$, with r_{ij} the distance to the nearest-neighbor oxygen ions. R_0 and b are parameters given in Ref. [25] for inorganic cobalt compounds. The results for the oxidation numbers Z_j are given in Table IV. They show that we can nominally ascribe valence 2+ for all the Co ions. This automatically gives a valence 4+ for the Sn ions to have an electronic balance of the structure.

The bond angles M-O-M are specified for each metal site in Table V. We remark that with the exception of Co3-O-Co1 and Co3-O2-Co4 these angles are near 90°.

C. Magnetic measurements

The magnetic measurements in powdered samples of $Co_5Sn(O_2BO_3)_2$ were carried out using a commercial PPMS platform from Quantum Design. The results of the magnetic measurements are shown in Figs. 2, 3, and 4.

Figure 2 shows the magnetization versus temperature curves for field-cooled (FC) and zero-field-cooled (ZFC) procedures, for the applied field of 0.1 T. Near 82 K the curves show an abrupt change of derivative and then the ZFC and FC curves separate. In zero field cooling, the ordered magnetic system breaks down in magnetic domains, as evidenced by the drop in the magnetization curves and consistent with the observation of dissipation in χ''_{ac} as described below. The temperature dependence of the inverse dc susceptibility is linear above 120 K, characteristic of the paramagnetic regime. Using a Curie-Weiss law fitting, as shown in the inset of Fig. 2, we obtain the Curie-Weiss temperature $\theta_{WC} = -32.5$ K and the Curie constant $C = 26.06 \times 10^{-3}$ emu K/g Oe. The θ_{WC} is near that, −25 K, obtained for the homometallic $Co_3O_2BO_3$ [13] and indicates the predominance of antiferromagnetic interactions in both systems. From the Curie constant we determine the effective moment per Co atom $p = g\sqrt{J(J+1)} = 4.98\ \mu_B$, which yields $J = 2.04$ considering $g = 2$. The magnetism of the $3d$ series is due mainly to the spin magnetic moment, with a small or null orbital contribution. The effective moment per ion, 4.98 μ_B, found here is consistent with that experimentally observed for Co^{2+} ions, namely 4.8 μ_B [28].

Figure 3 shows ac-susceptibility measurements for different frequencies as a function of temperature. The real part of χ_{ac} shows a sharp peak at the temperature $T_N = 82$ K, which we identify as the Néel temperature of the material. The variation of T_N with frequency for two decades is smaller than 0.2 K, which implies that this transition is not due to dynamic effects as in glassy systems. It is a well-defined thermodynamic transition as confirmed by specific-heat results to be shown later. We remark that this temperature is almost two times higher than that obtained for $Co_3O_2BO_3$ [13], 43 K. The imaginary part of χ_{ac}, but not the onset of dissipation, shows

TABLE IV. Oxidation numbers for the cobalt ions in $Co_5Sn(O_2BO_3)_2$ obtained by the method of Wood and Palenik (Ref. [25]) from the distances appearing in Table III (see text).

Co1	1.806
Co2	1.806
Co3	1.818
Co4	1.956

TABLE V. The M-O-M bond angles in degrees for $Co_5Sn(O_2BO_3)_2$. The subscript is the symmetry code $(i)\ x-1/2, -y+1/2, z$.

Co1-O2-Co4	99.12(6)
Co2-O3-Co3	93.69(5)
Co3-O2-Co1	121.14(7)
Co3-O2-Co4	117.11(5)
Co3-O4-$Co4_i$	99.76(6)
$Co4_i$-O4-Co2	83.77(2)
Co4-O1-Co1	92.27(5)
$Co4_i$-O5-Co3	95.49(5)

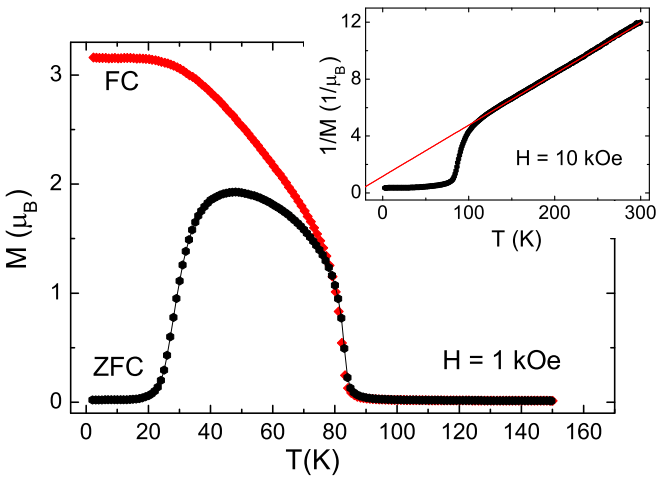

FIG. 2. (Color online) Magnetization versus temperature for $Co_5Sn(O_2BO_3)_2$ under an applied field of 0.1 T in both regimes: field cooled (FC) and zero field cooled (ZFC). The inset shows the inverse of the ZFC magnetization curve for an applied magnetic field of 1 T.

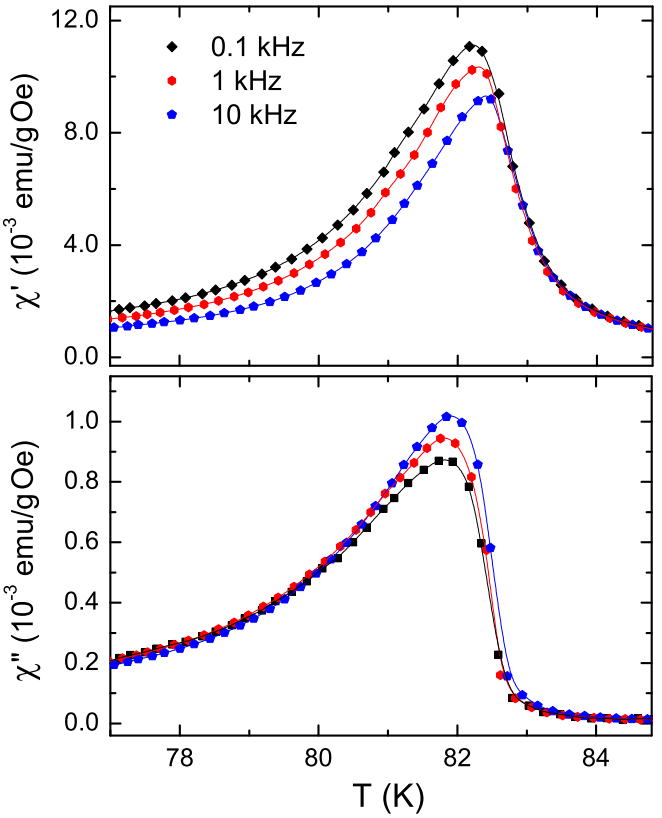

FIG. 3. (Color online) Real (χ') and imaginary (χ'') parts of $Co_5Sn(O_2BO_3)_2$ ac magnetic susceptibility as functions of temperature for 0.1 kHz, 1 kHz, and 10 kHz. The amplitude of the oscillating magnetic field is 1 Oe.

a frequency dependence as expected from the formation of domain walls in the ordered magnetic phase.

The magnetization curves as functions of applied fields for different temperatures are shown in Fig. 4. At 100 K the magnetization exhibits a paramagnetic behavior. Below

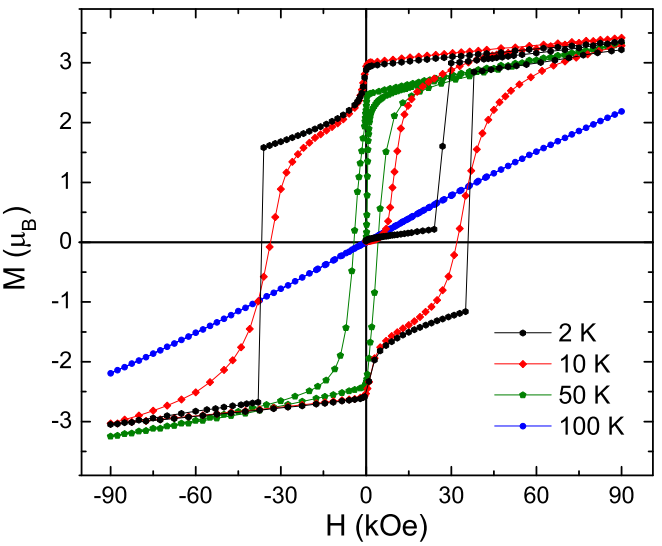

FIG. 4. (Color online) $Co_5Sn(O_2BO_3)_2$ magnetization versus applied magnetic field curves at 2, 10, 50, and 100 K.

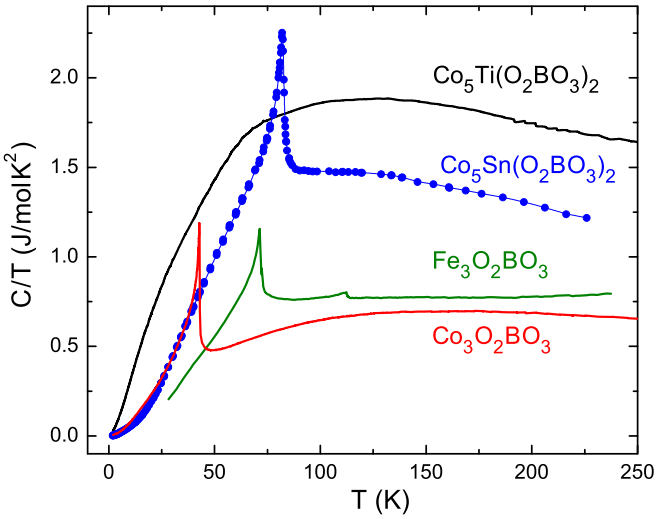

FIG. 5. (Color online) Specific heat of the ludwigite $Co_5Sn(O_2BO_3)_2$, plotted as C/T versus T (present work), compared with the results for other ludwigites taken from Refs. [9,13,16].

T_N the magnetization versus field curves present hysteresis cycles down to the lowest reached temperatures. Below 10 K these curves present small jumps at low fields and, near 2 K, a sharp one at 3.8 T. This behavior was also found in $Co_5Ti(O_2BO_3)_2$ [16] and in this case related to a spin-glass phase [29]. However, contrary to the $Co_5Ti(O_2BO_3)_2$ system, for which the specific heat as a function of temperature does not present any feature, here it has a narrow peak characteristic of a well-defined thermodynamic transition. This excludes a spin-glass transition in the present system, differently from what was found in the former. The magnetization jumps found in the M versus H measurements shown in in Fig. 4 are associated with metamagnetic behavior. They should be linked to a rearrangement of the magnetic configuration due to the competition between the Zeeman energy and the magnetic anisotropy present in this material. It reinforces the complex nature of the interactions, and consequently of the magnetic order, in this compound.

D. Specific-heat measurements

Specific-heat measurements as a function of temperature and magnetic field were performed employing 11.3 mg of randomly oriented crystalline needles. Results are shown in Figs. 5 and 6.

Figure 5 shows the specific-heat curves plotted as C/T versus T for different ludwigites: $Co_5Sn(O_2BO_3)_2$ (present work), $Co_5Ti(O_2BO_3)_2$ [16], $Co_3O_2BO_3$ [13], and $Fe_3O_2BO_3$ [9]. The two homometallic ludwigites $Co_3O_2BO_3$ and $Fe_3O_2BO_3$ present sharp peaks at 42 K and 70 K, respectively, showing the magnetic order of the whole system. $Fe_3O_2BO_3$ has still another small peak due to a partial magnetic order of the Fe^{3+} ions [9]. In the ludwigites doped by nonmagnetic ions the magnetic order is diminished or suppressed like in $Co_5Ti(O_2BO_3)_2$. The $Co_5Sn(O_2BO_3)_2$ system has a sharp peak at 81.5 K similar to that observed in the homometallic ludwigites. This peak together with the results of the magnetic measurements suggests that this compound has a ferrimagnetic

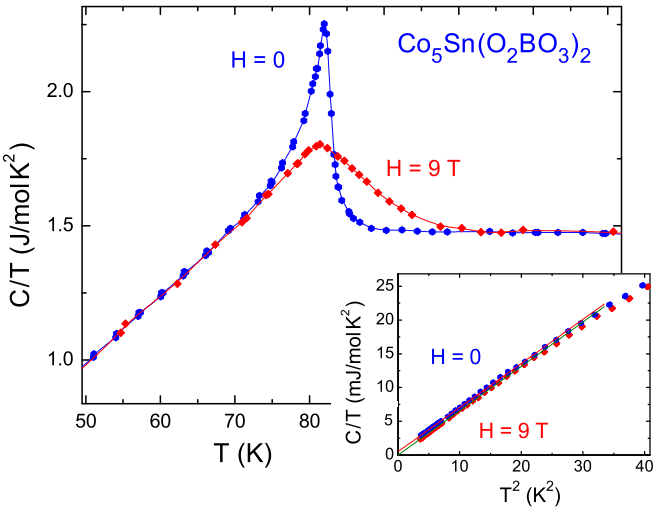

FIG. 6. (Color online) $Co_5Sn(O_2BO_3)_2$ specific heat plotted as C/T versus T for applied fields of 0 T and 9 T. The inset show the low temperature of C/T versus T^2 curve for applied fields of 0 T and 9 T. The linear behavior below approximately 5 K shows that the curves can be described by the equation $C/T = \gamma + \beta T^2$. The values of γ and β obtained from the fits are in Table VI.

transition near 82 K. Contrary to other ludwigites doped with nonmagnetic ions, Sn doping enhances the magnetic order, such that the magnetic transition in $Co_5Sn(O_2BO_3)_2$ is even higher than that of the homometallic compound. Figure 6 shows the specific-heat curves of $Co_5Sn(O_2BO_3)_2$, plotted as C/T versus T, with and without an applied magnetic field of 9 T. We notice that the peak at 82 K smooths down but does not shift with the applied magnetic field. This was also observed in the $Co_3O_2BO_3$ [13] and indicates a type of magnetic order more complex than that of a conventional antiferromagnet. It is possible that the field polarizes the spins on both sides of the transition reducing the variation of entropy. This also reinforces the ferrimagnetic nature of our sample.

At the lowest temperatures we fitted (see inset of Fig. 6) the low-temperature specific heat using a $C/T = \gamma + \beta T^2$ law. This yields the parameters shown in Table VI. The T^3 term in solids is generally due to lattice excitations and we can extract the Debye temperature θ_D using the formula $\theta_D^3 = 234R/\beta$, where R is the universal gas constant [28]. The θ_D of $Co_5Sn(O_2BO_3)_2$ is of the same order of magnitude as that obtained for $Co_3O_2BO_3$ (see Table VI), while the γ parameter is much smaller than in the others ludwigites. This linear term is usually attributed to charge carriers, as free electrons in a Fermi liquid. The oxyborates are generally semiconductors at low temperatures but, in principle, this term could arise from itinerant electrons in the three-leg ladders in the mixed-valent ludwigites [13]. We note that the values of γ obtained for the first two ludwigites in Table VI are of the order of that found in simple metals, such as K (K = 2.08 mJ/mol K^2) or Pb (Pb = 2.98 mJ/mol K^2) [28], and not so dependent on the magnetic field.

TABLE VI. The γ and β parameters obtained from the fit $C/T = \gamma + \beta T^2$ of the very low temperature specific heat measurements. The β coefficient yields the effective Debye temperature θ_D, using $\theta_D^3 = 234R/\beta$ where R is the universal constant gas. H is the applied magnetic field and "pw" means present work.

	H (T)	γ (mJ/mol K^2)	β (mJ/mol K^4)	θ_D (K)	Ref.
$Co_3O_2BO_3$	0	3.30	0.72	139	[13]
$Co_3O_2BO_3$	9	3.48	0.70	140	[13]
$Co_2FeO_2BO_3$	0	3.28	0.23	204	[10]
$Co_5Ti(O_2BO_3)_2$	0	15.03	3.94	79	[16]
$Co_5Ti(O_2BO_3)_2$	3	6.88	2.78	89	[16]
$Co_5Ti(O_2BO_3)_2$	9	3.61	2.76	89	[16]
$Co_5Sn(O_2BO_3)_2$	0	0.54 ± 0.02	0.650 ± 0.002	144	pw
$Co_5Sn(O_2BO_3)_2$	9	0.00 ± 0.02	0.656 ± 0.002	143	pw

A linear temperature dependent specific heat is also observed in spin glasses [29], which have magnetic frustration, such as $Co_5Ti(O_2BO_3)_2$. In this case, values of γ can also be high and present a strong magnetic field dependence. For the present $Co_5Sn(O_2BO_3)_2$ system, the linear contribution to the specific heat turns out to be very small as can be seen in Table VI. According to our x-ray and Mössbauer data (see below) the $Co_5Sn(O_2BO_3)_2$ only has Co^{2+} ions. Then, since this system has no mixed-valency, we can expect the electronic contribution to the linear specific heat to be negligible. On the other hand the experimental finding of negligible γ shows that the present material has fewer competing interactions and consequently a smaller degree of frustration when compared to the other ludwigites. This is consistent with the existence of long-range magnetic order (as opposed to spin-glass ordering) and the observed enhancement of the ordering temperature of this system.

E. Mössbauer spectroscopy

The Mössbauer spectroscopy of ^{119}Sn was performed between 4.2 K and 300 K in transmission geometry. The spectra were taken with the ^{119m}Sn:$CaSnO_3$ source and the powdered sample maintained at the same temperature in an Oxford Cryosystems device, moving in a sinusoidal mode. The spectra were least-squares fitted using the NORMOS program and the isomer shift values are in relation to $BaSnO_3$. The Mössbauer spectra of ^{119}Sn of $Co_5Sn(O_2BO_3)_2$ and the hyperfine parameter for different temperatures are shown in Fig. 7 and Table VII. For the fit of the paramagnetic spectra (300 K and 84 K) only one doublet was used. The observed linewidth of $G = 0.85$ mm/s is in reasonable agreement with the theoretical value of 0.64 mm/s (Ref. [27]), indicating that Sn ions occupy only one type of site, in agreement with the x-ray data presented above. The isomer shift value $\delta = 0.2$ mm/s is consistent with an oxidation state of 4+ for Sn [27]. As is evident from the ^{119}Sn Mössbauer spectra shown in Fig. 7, below 82 K the spectra begin to broaden magnetically indicating the onset of the magnetic transition according to the transition temperature obtained by the magnetic and transport measurements. Below 82 K the spectra were fitted with two magnetic components. The quadrupole splitting ΔE_Q, isomer shift δ, sign of V_{ZZ} (main component of the electrical field gradient tensor), hyperfine magnetic field B_{hf}, and angle θ between the directions of B_{hf} and V_{ZZ} were the free fitting parameters. Between 82 K $\leqslant T \leqslant$ 80 K the main component

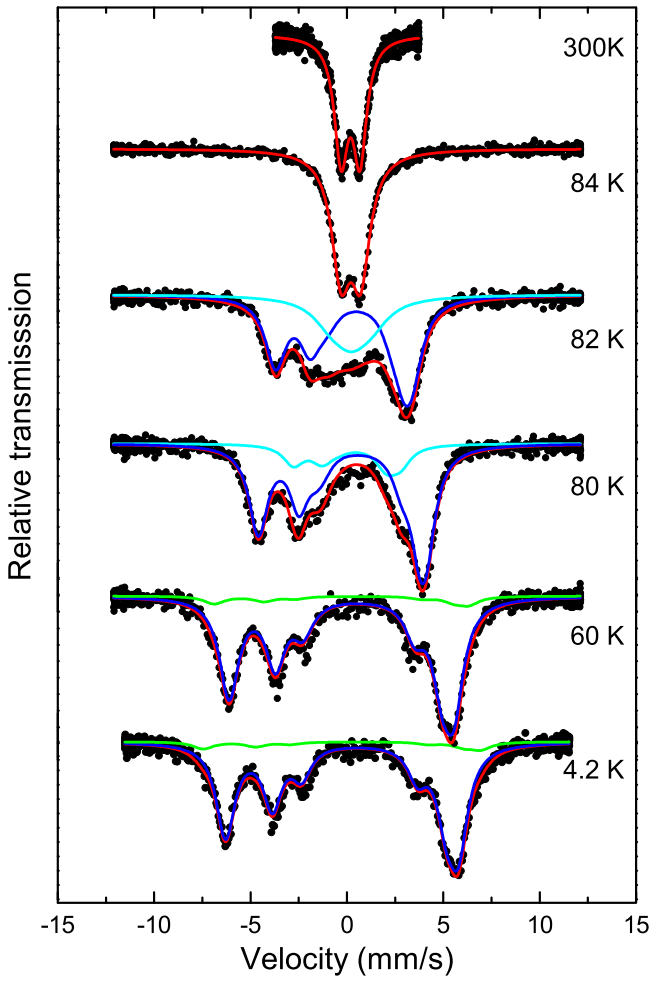

FIG. 7. (Color online) Some ^{119}Sn Mössbauer spectra of $Co_5Sn(O_2BO_3)_2$ in the temperature range of 300 K $\leqslant T \leqslant$ 4.2 K. Between 300 K $\leqslant T \leqslant$ 84 K only one doublet was used to fit the spectra. Below 82 K all the spectra were fitted with two magnetic subspectra.

corresponds to the ions in a static magnetic state (blue line) and the minor one to the ions in a magnetic relaxation state, due to a short-range interaction near the transition temperature, or to a state with a not well defined direction (cyan line). Below 80 K only the static magnetic components survive. Since Sn is not a transition element, it does not have a magnetic hyperfine field in the nucleus created by the unfilled 3*d* orbitals in its own electronic layer. So the magnetic hyperfine field on the Sn nucleus is a transferred magnetic field due to the magnetic moments of the neighbor Co ions. At 60 K the B_{hf} almost reach the saturation value (see Table VII) and below this temperature the spectra were fitted with two magnetic subspectra. The sextet with an absorption area of 92.6% is attributed to the Sn in the site 4. The other subspectra, corresponding to a 7.6% of the total area, can be due to the Sn at the site 4 in a special configuration, like clusters, or due to a small percentage of Sn at site 2. This small fraction of Sn is not observed in the paramagnetic spectra (where only electric interactions take place) probably due the crystallographic similarity of sites 2 and 4 which can generate almost the same quadrupole splitting.

TABLE VII. Mössbauer hyperfine parameter of $Co_5Sn(O_2BO_3)_2$ for temperatures between 300 and 4.2 K. The parameters are the temperature T, isomer shift δ, quadrupole splitting ΔE_Q, linewidth Γ, hyperfine magnetic field B_{hf}, angle θ between the B_{hf} and the principal axis of the electrical gradient field V_{ZZ}, and the absorption area A.

T (K)	δ (mm/s)	ΔE_Q (mm/s)	Γ (mm/s)	B_{hf} (T)	θ (°)	A (%)
300	0.21	0.97	0.85			100
87	0.20	1.01	1.00			100
84	0.21	1.02	1.18			100
82	0.18	0.97	1.30	5.15	16.2	67.4
	0.22	−1.01	2.20	1.01	55.0	32.6
80	0.20	−1.06	1.18	6.44	11.2	79.5
	0.22	−0.94	1.30	3.88	27.1	20.5
60	0.17	−0.97	1.20	8.72	10.0	92.4
	0.17	−0.91	1.30	9.94	0	7.6
40	0.20	−0.94	1.28	9.00	0	92.4
	0.18	−0.92	1.30	11.00		7.6
20	0.18	−0.94	1.24	9.05	0	92.4
	0.20	−0.94	1.30	11.07		7.6
4.2	0.20	−0.91	1.20	9.08	0	92.4
	0.20	−0.90	1.20	10.83	0	7.6

III. DISCUSSION

In this work we reported the synthesis and a quite complete characterization of the system $Co_5Sn(O_2BO_3)_2$ using x-ray diffraction, Mössbauer spectroscopy, and magnetization and specific-heat measurements. The Sn ions replace the Co ions only in the site 4 of the ludwigite structure (Fig. 1) in almost equal proportion, as indicated by the x-ray diffraction and Mössbauer spectroscopy. By using the x-ray data we calculated the valence 2+ for all the Co ions using the bond valence sum method. The Mössbauer spectroscopy of ^{119}Sn confirms the oxidation state 4+ obtained for Sn. On average, it keeps the site 4 with valence 3+; this seems to be a characteristic of all the ludwigites. We did not find any evidence for a structural transition to temperatures as low as 110 K. The presence of nonmagnetic ions in other cobalt ludwigites diminishes the magnetic interactions as evidenced by the smaller transition temperatures, as in $Co_{3-x}Ga_xO_2BO_3$ [18] ($T_o = 37$ K), or destroys completely the order in favor of a spin-glass state like in $Co_5Ti(O_2BO_3)_2$ [16] ($T_{sg} = 19$ K) and $CoMgGaO_2BO_3$ [17] ($T_{sg} = 25$ K). The $Co_5Sn(O_2BO_3)_2$ system has long-range magnetic order below $T_N \approx 82$ K as shown by narrow peaks in the specific-heat and susceptibility measurements (see Figs. 3 and 5). Surprisingly the magnetic interactions are strengthened by the introduction of nonmagnetic ions and the transition temperature of the whole system is the highest found among the ludwigites. On the other hand, the strength of the magnetic anisotropy can be gauged by the low-temperature coercive field, $H_{coercive} \approx 4$ T, obtained by magnetization measurements shown in Fig. 4. The coercive field found in $Co_3O_2BO_3$ is near 2 T [13], almost half the value of the present system, as is also the case for the transition temperature, 43 K. In the ludwigites there is a competition between three types of magnetic interactions: direct exchange, superexchange, and double exchange. In $Co_5Sn(O_2BO_3)_2$ the

latter should not be present since the magnetic ions do not have mixed valence in this material. The volume of the cell is the highest compared to other ludwigites cited in this paper, which gives higher distances between the metal ions. Direct exchange is usually possible in the 4-2-4 ladders which have the smallest intermetallic distances. For $Co_5Sn(O_2BO_3)_2$ this distance is 2.8338(1) Å that is higher compared to the homometallic compounds, 2.7510(4) Å for $Co_3O_2BO_3$ [13] and 2.786(1) Å for $Fe_3O_2BO_3$ [2]. Thus the magnetism of this system shall be governed essentially by superexchange interactions. This seems to reduce competition and reinforce long-range magnetic order. The small γ parameter which vanishes in an applied magnetic field (see Table VI) corroborates the absence of frustration and of a feeble competition between the magnetic interactions. Although the compound has θ_{WC} negative, which indicates predominance of antiferromagnetic interactions, the ground state is not a conventional antiferromagnet. This is shown by the effect of the external magnetic field in the peak of the specific heat that is not shifted to low temperatures as would be expected. There are ferromagnetic interactions, as we can see by the magnetization curves in Fig. 2 and also by the hysteresis below T_N in Fig. 4. These figures are very similar to those of $Co_3O_2BO_3$, with the exception of the discontinuities found in the magnetization versus field curves of $Co_5Sn(O_2BO_3)_2$ below 10 K. It reveals the ferrimagnetic nature of both compounds. The jumps in the hysteresis curves arise due to the competition between the Zeeman energy due to the external magnetic field and the strong magnetic anisotropy of this material, but they need to be studied in more detail.

IV. CONCLUSIONS

Oxyborates of the ludwigite type present a variety of interesting properties related to the existence of low-dimensional structures existing in this class of compounds [1]. The majority of the ludwigites have mixed valence and a competition between magnetic interactions as double and direct exchange and superexchange. $Co_5Sn(O_2BO_3)_2$ is the unique ludwigite where the double exchange seems to be absent. The compound has a ferrimagnetic transition near 82 K. In spite of being doped with nonmagnetic ions, this critical temperature is the highest found in the ludwigites for a magnetic ordering of the whole system. The absence of double-exchange interactions accounts for this record. The magnetic mechanism responsible for magnetic ordering in $Co_5Sn(O_2BO_3)_2$ seems to be more simple than that involved in other ludwigites. A complete understanding of this mechanism can help to understand many properties found in other ludwigites. We hope this study will motivate further experimental and theoretical work in these interesting materials.

ACKNOWLEDGMENT

Support from the Brazilian agencies CNPq and Fundação de Amparo a Pesquisa do Estado do Rio de Janeiro - FAPERJ is gratefully acknowledged.

[1] M. A. Continentino, J. C. Fernandes, R. B. Guimarães, B. Boechat, and A. Saguia, in *Frontiers in Magnetic Materials*, edited by A. V. Narlikar (Springer, Berlin, 2005), pp. 385–410.

[2] M. Mir, R. B. Guimarães, J. C. Fernandes, M. A. Continentino, A. C. Doriguetto, Y. P. Mascarenhas, J. Ellena, E. E. Castellano, R. S. Freitas, and L. Ghivelder, Phys. Rev. Lett. **87**, 147201 (2001).

[3] P. Bordet and E. Suard, Phys. Rev. B **79**, 144408 (2009).

[4] J. P. Attfield, A. M. T. Bell, L. M. Rodriguez-Martinez, J. M. Greneche, R. J. Cernik, J. F. Clarke, and D. A. Perkins, Nature (London) **396**, 655 (1998).

[5] M. Angst, P. Khalifah, R. P. Hermann, H. J. Xiang, M. H. Whangbo, V. Varadarajan, J. W. Brill, B. C. Sales, and D. Mandrus, Phys. Rev. Lett. **99**, 086403 (2007).

[6] M. Angst, R. P. Hermann, W. Schweika, J.-W. Kim, P. Khalifah, H. J. Xiang, M.-H. Whangbo, D.-H. Kim, B. C. Sales, and D. Mandrus, Phys. Rev. Lett. **99**, 256402 (2007).

[7] R. J. Goff, A. J. Williams, and J. P. Attfield, Phys. Rev. B **70**, 014426 (2004).

[8] R. B. Guimarães, M. Mir, J. C. Fernandes, M. A. Continentino, H. A. Borges, G. Cernicchiaro, M. B. Fontes, D. R. S. Candela, and E. Baggio-Saitovitch, Phys. Rev. B **60**, 6617 (1999).

[9] J. C. Fernandes, R. B. Guimarães, M. A. Continentino, L. Ghivelder, and R. S. Freitas, Phys. Rev. B **61**, R850 (2000).

[10] D. C. Freitas, M. A. Continentino, R. B. Guimarães, J. C. Fernandes, E. P. Oliveira, R. E. Santelli, J. Ellena, G. G. Eslava, and L. Ghivelder, Phys. Rev. B **79**, 134437 (2009).

[11] T. G. Rappoport, L. Ghivelder, J. C. Fernandes, R. B. Guimarães, and M. A. Continentino, Phys. Rev. B **75**, 054422 (2007).

[12] D. C. Freitas, R. B. Guimarães, J. C. Fernandes, M. A. Continentino, C. B. Pinheiro, J. A. L. C. Resende, G. G. Eslava, and L. Ghivelder, Phys. Rev. B **81**, 174403 (2010).

[13] D. C. Freitas, M. A. Continentino, R. B. Guimarães, J. C. Fernandes, J. Ellena, and L. Ghivelder, Phys. Rev. B **77**, 184422 (2008).

[14] N. B. Ivanova, A. D. Vasiliév, D. A. Velikanov, N. V. Kazak, S. G. Ovchinnikov, G. A. Petrakovskii, and V. V. Rudenko, Phys. Solid State **49**, 651 (2007).

[15] N. V. Kazak, N. B. Ivanova, V. V. Rudenko, A. D. Vasil'ev, D. A. Velikanov, and S. G. Ovchinnikov, Phys. Solid State **51**, 966 (2009).

[16] D. C. Freitas, R. B. Guimarães, D. R. Sanchez, J. C. Fernandes, M. A. Continentino, J. Ellena, A. Kitada, H. Kageyama, A. Matsuo, K. Kindo, G. G. Eslava, and L. Ghivelder, Phys. Rev. B **81**, 024432 (2010).

[17] N. B. Ivanova, M. S. Platunov, Yu. V. Knyasev, N. V. Kazak, L. N. Bezmternykh, A. D. Vasiliev, S. G. Ovchinnikov, and V. I. Nizhankovskii, Low Temp. Phys. **38**, 172 (2012).

[18] N. B. Ivanova, M. S. Platunov, Yu. V. Knyasev, N. V. Kazak, L. N. Bezmternykh, E. V. Eremin, and A. D. Vasiliev, Phys. Solid State **54**, 2212 (2012).

[19] CrysAlisPro, Oxford Diffraction Ltd., Version 1.171.33.41 (release 06-05-2009 CrysAlis 171.NET).
[20] R. C. Clark and J. S. Reid, Acta Cryst. **A51**, 887 (1995).
[21] SHELXS97: Program for Crystal Structure Solution (release 97-2). G. M. Sheldrick, Institüt für Anorganische Chemie der Universität, Tammanstrasse 4, D-3400 Göttingen, Germany, 1998.
[22] SHELXL97: Program for Crystal Structure Refinement (release 97-2). G. M. Sheldrick, Institüt für Anorganische Chemie der Universität, Tammanstrasse 4, D-3400 Göttingen, Germany, 1998.
[23] L. J. Farrugia, J. Appl. Cryst. **32**, 837 (1999).
[24] G. Bergherhoff, M. Berndt, and K. Brandenburg, Res. Natl. Inst. Stand. Technol. **101**, 221 (1996).
[25] R. M. Wood and G. J. Palenik, Inorg. Chem. **37**, 4149 (1998); D. C. de Freitas, M.Sc. thesis, Universidade Federal Fluminense, 2007.
[26] *International Tables for Crystallography*, Vol. A, edited by Theo Hahn, 5th ed., published for the International Union of Crystallography (Springer, Dordrecht, 2005), p. 283.
[27] N. N. Greenwood and T. C. Gibb, *Mossbauer Spectroscopy* (Chapman and Hall Ltd., London, 1971).
[28] C. Kittel, *Introduction to Solid State Physics*, 5th ed. (Wiley, New York, 1976), pp. 167, 426; J. M. D. Coey, *Magnetism and Magnetic Materials* (Cambridge University Press, Cambridge, UK, 2010), pp. 114–115.
[29] K. H. Fischer and J. A. Hertz, *Spin Glasses*, Cambridge Studies in Magnetism, No. 1 (Cambridge University Press, Cambridge, UK, 1993).